 doi:10.20944/preprints202208.0358.v1

Article

A Novel Trajectory Planning Method for Parafoil Airdrop System Based on Geometric Segmentation Strategy

Haitao Gao [1] and Jin Tao [2,*]

[1] College of Electrical and Electronic Engineering, Anhui Science and Technology University, Bengbu 233030, China; gaoht@ahstu.edu.cn;
[2] College of Artificial Intelligence, Nankai University, Tianjin 300350, China; taoj@nankai.edu.cn
* Correspondence: taoj@nankai.edu.cn; Tel.: +86-1831-025-9273

Abstract: Reasonable trajectory planning is the precondition for the parafoil airdrop system to achieve autonomous accurate homing, and safe landing. To successfully realize the self-homing of the parafoil airdrop system, a new trajectory optimization design scheme is proposed in this paper. The scheme is based on the parafoil's unique flight and control characteristics and adopts a segmented homing design. Compared with the current common trajectory design method, its core feature is to avoid the problem that the straight-line flight distance before landing is limited by the radius of the height-reducing area and ensures landing accuracy and safety. Firstly, the different starting states of the parafoil airdrop system and the landing requirements were comprehensively considered, and the homing trajectory is reasonably segmented. Based on the requirements of energy control, stable flight, and landing accuracy, the optimal objective function of the trajectory was established, and the trajectory parameters, calculation methods, and constraints were given. Secondly, the cuckoo search algorithm was applied to optimize the objective function to obtain the final home trajectory. Finally, the trajectory planning under different airdrop conditions was simulated and verified. The results showed that the planned trajectories could reach the target point accurately and meet the flight direction requirements, proving the proposed scheme's correctness and feasibility.

Keywords: trajectory planning; optimal control; parafoil; airdrop system; cuckoo search; geometric segmentation strategy

1. Introduction

The parafoil is controllable. Compared with the traditional circular parachute airdrop system, the airdrop system composed of the parafoil can achieve a precise airdrop of fixed-point targets under the controller's action. The parafoil airdrop system has a wide range of application values, such as the airdrop of relief materials in a disaster environment, the efficient delivery of military materials such as weapons and ammunition in the combat area, and the accurate recovery of spacecraft [1]. For example, in June 2021, China successfully recovered the Chang San Yi rocket booster through its recovery system. Similar to other unmanned aerial vehicles, the parafoil airdrop system also needs to track the planned trajectory when it realizes the autonomous homing operation [2-5]. Therefore, scientifically planning a high-quality homing trajectory is the premise for the parafoil airdrop system to achieve reliable autonomous flight. It is also an essential guarantee for the final realization of an accurate and safe airdrop [6-9].

The parafoil airdrop system is a soft-wing system, and its flight is easily disturbed by the surrounding environment, such as terrain and wind [10]. It is a nonlinear system and has many restrictions on its control. Therefore, various conditions and constraints must be considered for its homing trajectory planning [11-13]. The research on the autonomous homing trajectory of the parafoil airdrop system mainly focuses on two aspects. On the one hand, the homing trajectory is designed based on optimal control, which is a method to obtain the optimal control law under the designed objective function and various given

 doi:10.20944/preprints202208.0358.v1

constraints. For example, based on the parafoil point-mass model, Refs. [14-16] established a combined objective function, which considers the shortest landing distance, headwind landing, and energy-saving conditions. Under the constraints of airdrop starting point, target point, and control quantity, the objective function was solved by the Gaussian pseudospectral method or improved genetic algorithm to obtain the optimal trajectory. In Refs [17, 18], the design method of the optimal trajectory under abnormal conditions was studied, which are the insufficient launch height of the parafoil airdrop system and the failure of the actuator of the control system during the homing process. The objective function and constraints were obtained, and the Gauss pseudospectral method received the control rate. Based on the point-mass model in the wind field environment, Luo et al. [19] studied the planning of the homing trajectory in complex areas such as multi-peak landforms, established an obstacle model, designed an objective function for multi-objective combined optimization, and obtained the optimal homing trajectory and control rate under given constraints. Considering an error between the traditional point-mass model in trajectory planning and the actual flight situation, Sun et al. [20-22] proposed a third-order trajectory optimization strategy based on the six-degree-of-freedom model.

From the above research, it is not difficult to see that the use of optimal control theory to solve the homing trajectory planning problem of the parafoil system achieved rich results, which are similar to the problem of traditional aircraft, including the application and improvement of optimal algorithm, homing environment, and condition limitation. It promotes the research depth of parafoil homing trajectory. However, the parafoil airdrop system usually does not have a power propulsion device, it cannot fly freely like the traditional aircraft, and the control amount needs to be kept within a small range to ensure the safe flight of the system. Trajectories designed by optimal theory often operate frequently on control quantities, especially in complex environments. Therefore, it is difficult to be used in practical engineering applications.

On the other hand, the trajectory planning of the parafoil airdrop system was segmentally planned. According to the unique flight characteristics of the parafoil system, the trajectory design is planned and implemented step by step from the initial release point to the target point according to specific rules, taking into account the design process. In the trajectory design process, performance indicators such as energy consumption, stability, and safety are taken into account to make the planned trajectory as optimal as possible. In Ref [23], the target point was set in the center of the hovering height elimination area, and the homing trajectory of the parafoil system was designed in sections. And the optimal solution of the objective function was solved through the AP-QDEA optimization algorithm proposed in the paper to determine the homing trajectory of each section. Ref [24] studied the segmental design of the homing trajectory of the parafoil system in the risk and obstacle avoidance environment and combined it with the optimal trajectory planning theory. A hybrid trajectory planning method was proposed to obtain the trajectory segments under different conditions. However, In the currently more common segmented trajectory design scheme, the target point is usually designed at the center point of the hovering area, which makes the length of the upwind gliding flight segment limited by the length of the radius of the hovering area when the airdrop system is landing and brings challenges to the accuracy and safety of landing.

The control rate of the parafoil airdrop system obtained according to the optimal control theory usually has frequent cross control of the left and right parafoil ropes when realized, increasing the difficulty in engineering practice. The segmented trajectory considers the characteristics of the parafoil at the beginning of the trajectory design, which has the advantage of being designed in advance. At the same time, the trajectory designed by this method is easier to realize in the actual tracking overcharge. Aiming at the shortcomings of the existing segmented flight trajectory, this paper improves the segmented method of the trajectory and proposes a new segmented flight trajectory design scheme, which provides a new reference for the autonomous homing flight of the parafoil airdrop system. The main contributions of this paper are as follows:

Preprints (www.preprints.org) | NOT PEER-REVIEWED | Posted: 19 August 2022 doi:10.20944/preprints202208.0358.v1

- Based on the geometric segmentation strategy, a new autonomous homing scheme for the parafoil airdrop system is designed. The straight-line flight segment before landing is designed on the tangent of the circle with reduced height, and its length can be freely controlled. Compared with the target point being developed at the center of the circle with reduced altitude, it avoids the problem that the length of the straight flight segment before landing is subject to the circling radius and provides a guarantee for the smooth implementation of a bird landing in terms of landing accuracy and safety;
- The objective function of trajectory optimization is established, and the calculation method and constraints of trajectory parameters are introduced in detail. And the realization process of the new method of trajectory planning is described with examples;
- Different initial conditions for airdrops are set, the trajectory planned by the new scheme is simulated and verified, and a comparative analysis and discussion with the traditional scheme are carried out, which proves the effectiveness of the trajectory planning scheme designed in this paper.

2. Construction of Point-mass Model of Airdrop System

The parafoil autonomous airdrop system generally consists of the parafoil, the load-carrying object, the object to be airdropped, and the controller [25, 26]. The parafoil airdrop system with an autonomous homing function does not have a power device. Its homing is realized by controlling the left and right pull-down parafoil ropes at the rear edge of the parafoil during its descent. The controller controls the servo mechanism that performs the pull-down action of the parafoil rope. When the parachute rope's pull-down amplitude on the parafoil's left side is more significant than that on the right side, the airdrop system performs a left turn flight. Instead, the airdrop system performs a right-turn flight. The airdrop system performs gliding flight when the left and right pulling amplitudes are equal. Through reasonable flight control by the controller, the parafoil airdrop system can achieve autonomous flight and airdrop materials to the designated destination.

Without external interference, the airdrop system drops steadily under the action of gravity and aerodynamic force. In order to ensure overall stability and safety, the moment of inertia is ignored, and the pull-down amplitude of one side of the parafoil rope must be kept within a small range. Therefore, the following settings are made in this paper:

- The horizontal speed v_s and vertical descent speed v_z of parafoil airdrop system are constant;
- Response without delay.

Based on the geodetic coordinate system, the point-mass motion equation of parafoil airdrop system is established, as shown in Equation (1), which is used for trajectory planning in the homing process of the system.

$$\begin{cases} \dot{x} = v_s \cos(\psi) + w_x \\ \dot{y} = v_s \cos(\psi) + w_y \\ \dot{\psi} = u \\ \dot{z} = v_z \end{cases}, \tag{1}$$

In Equation (1), (x, y, z) is the position of the system, u is the control quantity, ψ is the turning angle, and (w_x, w_y) is the transverse wind speed of the space where the system is located. The wind is usually greatly affected by the airdrop environment, and the parafoil airdrop system has relatively high requirements for the airdrop environment. Therefore, generally, only the impact of the average wind field on the parafoil flight is considered. For the convenience of research, the impact of the average wind field is usually converted into the trajectory tracking error, and only the effect of the wind direction is considered. This paper also follows this treatment method. That is $(w_x, w_y) = (0,0)$, the point-mass model of a can be further simplified, as shown in Equation (2),

Preprints (www.preprints.org) | NOT PEER-REVIEWED | Posted: 19 August 2022 doi:10.20944/preprints202208.0358.v1

$$\begin{cases} \dot{x} = v_s \cos(\psi) \\ \dot{y} = v_s \cos(\psi) \\ \dot{\psi} = u \\ \dot{z} = v_z \end{cases}. \quad (2)$$

3. Design of Homing Trajectory

The parafoil airdrop system itself does not have a power device. By controlling the two pull-down parachute ropes on the left and right of the trailing edge, the parafoil can homing autonomously. The entire segmented homing process can generally be divided into three parts: centripetal, energy control, and landing, as shown in Figure 1.

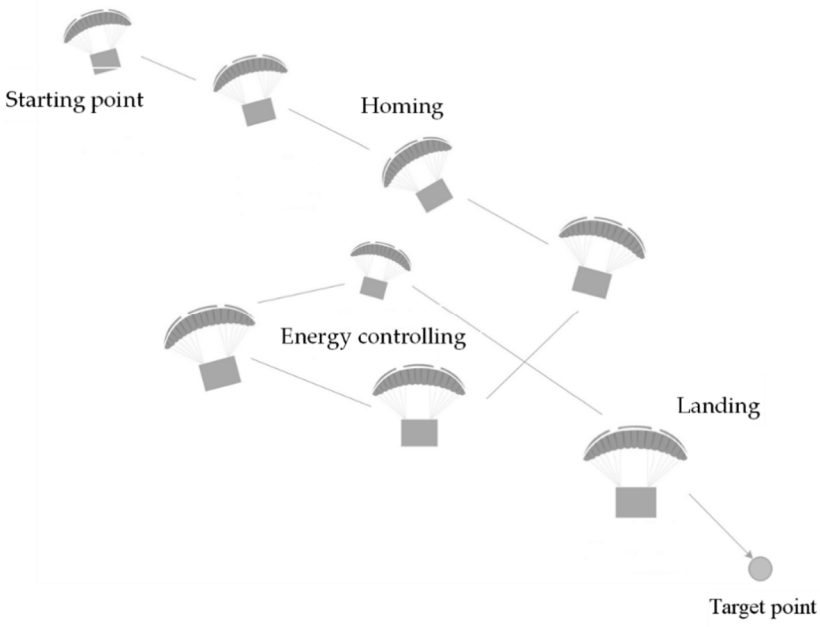

Figure 1. Homing process of parafoil airdrop system.

The centripetal flight is used to reduce the distance difference between the airdrop system and the target point; the capability control flight is used to eliminate the high degree of redundancy existing in the airdrop system; the landing flight is mainly used to adjust the flight direction, which is prepared for the windward landing of the airdrop system.

3.1. Trajectory Design Scheme

Based on the classical segmented trajectory design, this paper designs a new trajectory planning scheme, which not only considers the energy loss generated in the homing process, homing accuracy, and the overall flight safety of the system but also takes into account the convenience of the bird landing operation. The specific scheme is shown in Figure 2.

Preprints (www.preprints.org) | NOT PEER-REVIEWED | Posted: 19 August 2022 doi:10.20944/preprints202208.0358.v1

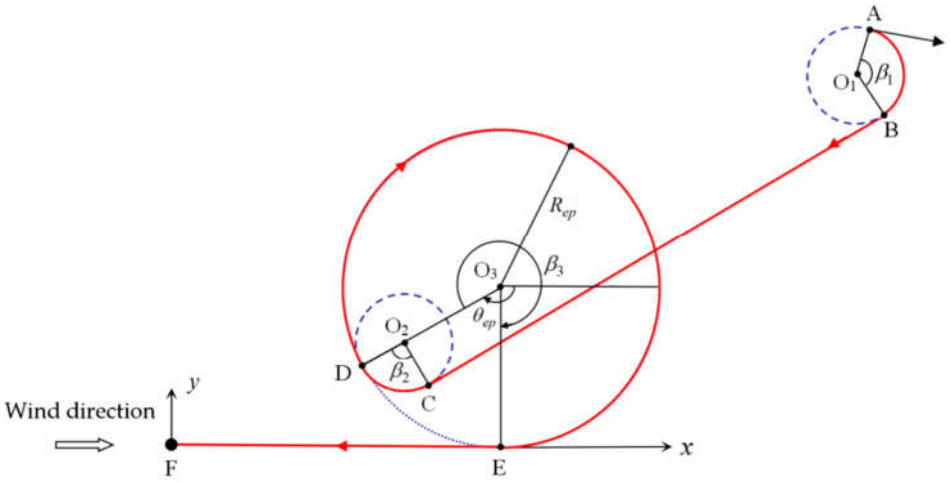

Figure 2. Diagram of trajectory design scheme.

In Figure 2, x and y are the two coordinate axes on the horizontal plane in the wind coordinate system. Axis z is perpendicular to plane x, y and intersects the plane x, y at point F, set the origin F of the wind coordinate system as the target point, and the wind direction is consistent with the x-axis direction. Point A is the starting point of the airdrop system after parachute opening. After turning through arc AB, the parafoil airdrop system flies to the circling area near the target point, and point D is the entry point. O_3 is the center of the circle in the circling area, and the parafoil airdrop system makes a turning flight around this point with R_{ep} as the radius, so as to reduce the flight altitude. θ_{ep} is the angle between the line connecting the two points D and O_3 and the positive direction of the x-axis. EF is the upwind flight phase before entering the bird's landing, and it is tangent to the circle O_3.

In order to reduce the control frequency of the controller and reduce the energy loss generated by it as much as possible, the trajectory in Figure 2 is designed with a single-side pull-down control method. When the parafoil system needs to adjust the flight direction, in order to achieve the purpose of fast and safe adjustment, make it turn with the minimum turning radius. As shown in Figure 1, the two arcs AB and CD are the flight direction adjustment sections, both of which are carried out with the minimum turning radius. The value range of the central angle corresponding to the two arcs is $0 \le \beta_1, \beta_2 \le \pi$, so as to reduce the control energy consumption as much as possible. The key to segment optimization is to determine the position of entry point D, which can be transformed into the calculation of the values of the two parameters R_{ep} and θ_{ep}. In order to make the whole planned trajectory optimal, the objective function shown in Equation (3) is established to obtain the optimal values of parameters R_{ep} and θ_{ep}.

$$\min J = \min\left|R_{\min} \cdot (\beta_1 + \beta_2) + (2k\pi + \beta_3) \cdot R_{ep} + \left\|\overrightarrow{BC}\right\| + \left\|\overrightarrow{EF}\right\| - f \cdot z_0\right|, \quad (3)$$

In Equation (3), J is the landing accuracy objective function, which represents the deviation between the landing point and the target point, where $R_{\min} \cdot (\beta_1 + \beta_2)$ represents the length of the arc AB and CD, $R_{ep} \cdot \beta_3$ represents the length of the arc DE, $\left\|\overrightarrow{BC}\right\|$ and $\left\|\overrightarrow{EF}\right\|$ represent the length of line segments BC and EF respectively, $f \cdot z_0$ represents the horizontal flight distance corresponding to the initial height of the parafoil system, and f is the glide ratio of the parafoil airdrop system.

3.2. Calculation and Constraints of Trajectory Parameters

Let (x_0, y_0, z_0) be the coordinates of the initial point, dir represents the turning flight direction of the parafoil system, $dir = -1$ is the clockwise flight, $dir = 1$ is the

Preprints (www.preprints.org) | NOT PEER-REVIEWED | Posted: 19 August 2022 doi:10.20944/preprints202208.0358.v1

counterclockwise flight, $L_{\mathrm{EF}} = \left\|\overrightarrow{EF}\right\|$, α_0 is the initial heading angle, and the center positions of β_1 and β_2 are represented by O_1 and O_2 respectively, then the vector $L_{\mathrm{O}_1\mathrm{O}_2}$ from O_1 to O_2 can be calculated by Equation (4),

$$\begin{aligned} L_{\mathrm{O}_1\mathrm{O}_2} &= \begin{vmatrix} x_{\mathrm{O}_1\mathrm{O}_2} \\ y_{\mathrm{O}_1\mathrm{O}_2} \end{vmatrix} \\ &= \begin{bmatrix} (R_{\mathrm{ep}} - R_{\min})\cos(\theta_{\mathrm{ep}}) \\ (R_{\mathrm{ep}} - R_{\min})\sin(\theta_{\mathrm{ep}}) \end{bmatrix} - \begin{bmatrix} x_0 + R_{\min} \cdot \cos\left(\alpha_0 + dir \cdot \frac{\pi}{2}\right) \\ y_0 + R_{\min} \cdot \sin\left(\alpha_0 + dir \cdot \frac{\pi}{2}\right) \end{bmatrix} + \begin{bmatrix} L_{\mathrm{EF}} \\ R_{\mathrm{ep}} \end{bmatrix} \end{aligned} \tag{4}$$

The included angle $\delta_{\mathrm{O}_1\mathrm{O}_2}$ between $L_{\mathrm{O}_1\mathrm{O}_2}$ and the positive direction of the x-axis can be calculated by Equation (5),

$$\begin{cases} \delta_{\mathrm{O}_1\mathrm{O}_2} = \mathrm{sign}\left(y_{\mathrm{O}_1\mathrm{O}_2}\right) \cdot \frac{\pi}{2}, & x_{\mathrm{O}_1\mathrm{O}_2} = 0 \\ \delta_{\mathrm{O}_1\mathrm{O}_2} = \frac{1 - \mathrm{sign}\left(x_{\mathrm{O}_1\mathrm{O}_2}\right)}{2} \cdot \pi \cdot \mathrm{sign}\left(y_{\mathrm{O}_1\mathrm{O}_2}\right) + \arctan\frac{y_{\mathrm{O}_1\mathrm{O}_2}}{x_{\mathrm{O}_1\mathrm{O}_2}}, & x_{\mathrm{O}_1\mathrm{O}_2} \neq 0 \end{cases}. \tag{5}$$

The included angles β_1, β_2 and β_3 of the circular arc in Figure 1 can be calculated by Equation (6) and Equation (7).

$$\begin{cases} \beta_1 = dir \cdot \left(\delta_{\mathrm{O}_1\mathrm{O}_2} - \alpha_0\right) \\ \beta_2 = dir \cdot \left(\alpha_2 - \delta_{\mathrm{O}_1\mathrm{O}_2}\right) \\ \beta_3 = dir \cdot \left(\frac{\pi}{2} - \theta_{\mathrm{ep}}\right) \end{cases}, \tag{6}$$

$$\Rightarrow \begin{cases} \beta_1 = \beta_1 + 2 \cdot \pi, & \beta_1 < 0 \\ \beta_2 = \beta_2 + 2 \cdot \pi, & \beta_2 < 0 \\ \beta_3 = \beta_3 + 2 \cdot \pi, & \beta_3 < 0 \end{cases}, \tag{7}$$

The parameter α_2 in Equation (6) can be obtained by Equation (8),

$$\begin{aligned} \alpha_2 &= \theta_{\mathrm{ep}} + dir \cdot \frac{\pi}{2} \\ &= \begin{cases} \alpha_2 - 2 \cdot \pi, & \alpha_2 > \pi \\ \alpha_2 + 2 \cdot \pi, & \alpha_2 \leq \pi \\ \alpha_2, & -\pi < \alpha_2 < \pi \end{cases}. \end{aligned} \tag{8}$$

In order to save the control energy as much as possible and improve the safety and stability of the airdrop system during flight, the value ranges of the agreed parameters R_{ep} and θ_{ep} are limited by Formula (9).

$$\begin{cases} R_{\mathrm{ep}} \in [R_1, R_2] \\ \theta_{\mathrm{ep}} \in (-\pi, \pi] \end{cases}. \tag{9}$$

In Formula (9), R_1 is the minimum turning radius allowed by the parafoil airdrop system when flying in the hovering high-flying area, corresponding to the maximum unilateral pull-down range of the parachute rope, and R_2 is the maximum turning radius.

4. Trajectory Optimization

The cuckoo search (CS) algorithm was proposed in 2009 [27]. It is a bionic algorithm generated by imitating the cuckoo's breeding and random flight behavior. The search process does not depend on the gradient and has the advantages of fewer parameters, high algorithm execution efficiency, and easy implementation. It has attracted the attention of many researchers. On this basis, many improved algorithms have been proposed to improve the overall performance of the algorithm [28-30], and base on the CS algorithm, combined with the piecewise trajectory design scheme proposed above, this paper searches for the optimal solution for the objective function shown in Equation (3) within

Preprints (www.preprints.org) | NOT PEER-REVIEWED | Posted: 19 August 2022 doi:10.20944/preprints202208.0358.v1

the given interval of parameters R_{ep} and θ_{ep}, and determines the trajectory. The specific implementation steps are shown in Figure 3.

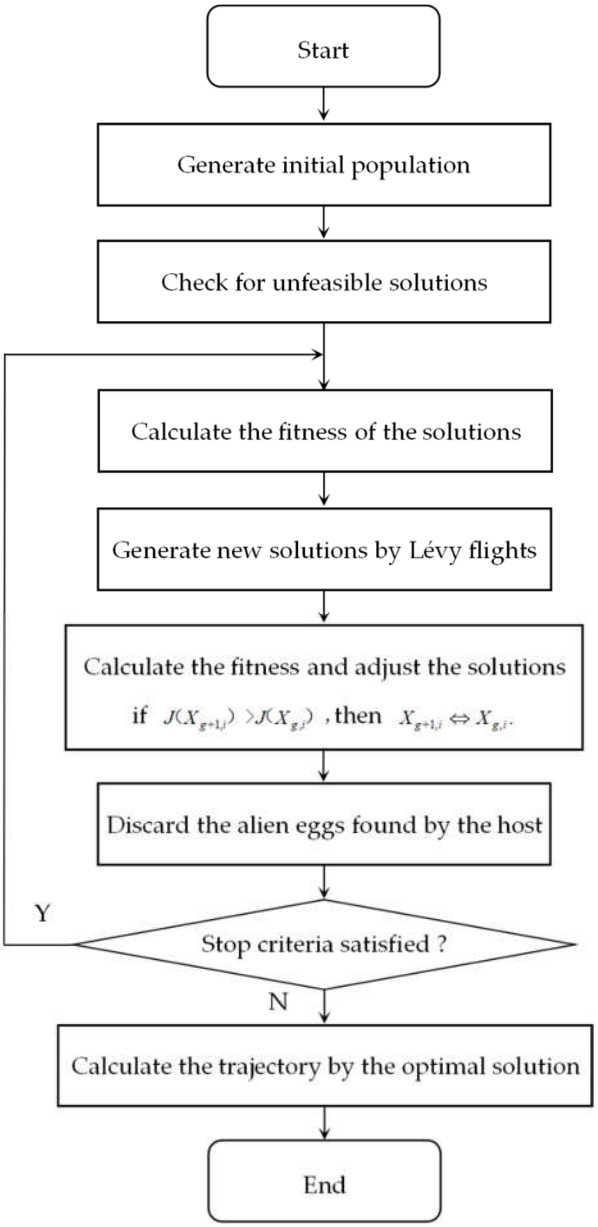

Figure 3. Flow chart of trajectory optimization.

Step 1: Initialize parameters such as population size N, the maximum number G_m of iterations, the probability P_a of the host discovering cuckoo eggs, the starting point coordinates (x_0, y_0, z_0), the initial direction α_0, the radius R_{ep} and the angle range θ_{ep} of the entry point, and other parameters. According to the value range shown in Formula (9), a two-dimensional initial population composed of R_{ep} and θ_{ep} is randomly generated, and its fitness value is calculated using the objective function shown in Equation (3).

Step 2: Generate a new levy flight solution from Equation (10). $X_{g,i}$ represents the i-th solution in the g-th generation, $Levy(\beta) \sim u_f / |v_f|^{1/\beta}$, $u_f \sim N(0, \sigma^2)$, $v_f \sim N(0,1)$, the parameter σ can be calculated by Equation (11),

$$X_{g+1,i} = X_{g,i} + \alpha \otimes Levy(\beta), \tag{10}$$

Preprints (www.preprints.org) | NOT PEER-REVIEWED | Posted: 19 August 2022 doi:10.20944/preprints202208.0358.v1

$$\sigma = \left\{ \frac{\sin(\beta \cdot \pi/2) \cdot \Gamma(1+\beta)}{\beta \cdot 2^{(\beta-1)/2} \cdot \Gamma((1+\beta)/2)} \right\}^{1/\beta}. \tag{11}$$

Step 3: Calculate the fitness value J of solution A, and update the solution set according to the following rules.

$$\text{if} \quad J(X_{g+1,i}) > J(X_{g,i}),$$

$$\text{then} \quad X_{g+1,i} \Leftrightarrow X_{g,i} \ .$$

Step 4: Update the solution set with the probability P_a of the host finding the cuckoo egg, as shown in Equation (12), where $H(\cdot)$ is the Heaviside step function, and $r, \varepsilon \sim U(0,1)$.

$$X_{g+1,i} = X_{g,i} + r \otimes H(P_a - \varepsilon) \otimes (X_{g,i} - X_{gj}). \tag{12}$$

Step 5: Calculate the fitness value of the solution set updated by Equation (12), and update the solution set using the rules in Step 3, find and save the optimal solution in the new solution set. Judge whether the search end condition is satisfied; if not, skip to step 2 for loop execution. Otherwise, end the loop and find the global optimal solution.

Step 6: Substitute the obtained optimal parameter (R_{ep}, θ_{ep}) into Equation (4)-(8) to calculate the parameters of each segment, and calculate the corresponding homing trajectory according to the initial conditions and the point-mass model of the parafoil airdrop system.

5 Simulation and Analysis

5.1. Parameter Setting

Table 1. Parameter setting

Parameter types	Parameters	Value (Unit)
Trajectory parameters	v_s	13.8 (m/s)
	v_z	4.6 (m/s)
	R_{min}	100 (m)
	R_1	200 (m)
	R_2	500 (m)
	$\|\overrightarrow{EF}\|$	100 (m)
	f	3
Optimization algorithm parameters	N	100
	G_m	200
	P_a	0.25
	α	1
	β	1.5

In order to prove the feasibility of the segmented trajectory planning scheme proposed in this paper, the trajectory optimization results are simulated and verified based on the point-mass model of the parafoil airdrop system and the cuckoo optimization algorithm. The relevant parameter settings in the trajectory optimization scheme and the cuckoo optimization algorithm are shown in Table 1.

In Table 1, the glide ratio f of the parafoil airdrop system is 3, its horizontal flight speed v_s is 13.8m/s, the vertical descent speed v_z is 4.6m/s, and the minimum turning radius R_{min} is set as 100m. Set the minimum R_1 and maximum R_2 of the radius R_{ep} of spiral height elimination as 100m and 500m, respectively. The headwind flight distance $\|\overrightarrow{EF}\|$ before bird landing is set as 100m. Let the number of nests N in the cuckoo optimization algorithm be 100. That is, the number of solutions is 100, the maximum number of

Preprints (www.preprints.org) | NOT PEER-REVIEWED | Posted: 19 August 2022 doi:10.20944/preprints202208.0358.v1

iterations G_m is 200, the probability P_a of the host discovering cuckoo eggs is 0.25, the step scaling factor α is 1, and β is 1.5.

5.2. Results and Analysis

The cuckoo optimization algorithm is used to solve the objective function shown in Equation (3), obtain the optimal solutions of R_{ep} and θ_{ep}, and then determine the optimal trajectory. In order to ensure the comprehensiveness of the verification, Table 2 shows three different airdrop situations, and the simulation analysis of their trajectory planning is carried out, respectively. The simulation results are shown in Figures 4-16.

Table 2. Initial state setting.

Initial state	x_0(m)	y_0(m)	z_0(m)	α_0(rad)
State 1	800	-650	1000	$-\pi/3$
State 2	800	650	1000	$-\pi/3$
State 3	800	650	2000	$-\pi/3$

5.2.1. Results of State 1

When the starting point of the parafoil airdrop system is at $(800\text{ m}, -650\text{ m}, 1000\text{ m})$, the optimal solution of the objective function is obtained through the cuckoo search algorithm, where $R_{ep} = 272.3363\text{rad}$, $\theta_{ep} = -3.1416\text{ rad}$, and the objective function value is 0 at this time. Figure 4 shows the convergence curve when the objective function is optimized. It can be seen that the curve converges when the search reaches 16 generations, and the convergence speed is faster.

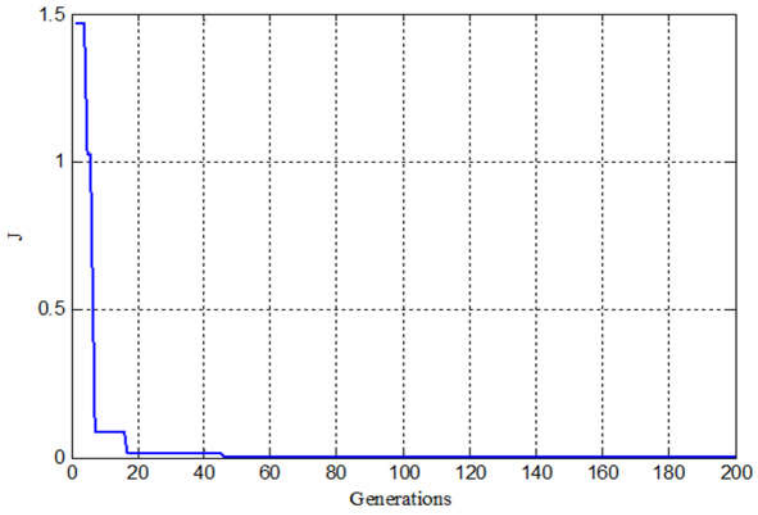

Figure 4. Convergence curve of the objective function under the state 1.

Preprints (www.preprints.org) | NOT PEER-REVIEWED | Posted: 19 August 2022 doi:10.20944/preprints202208.0358.v1

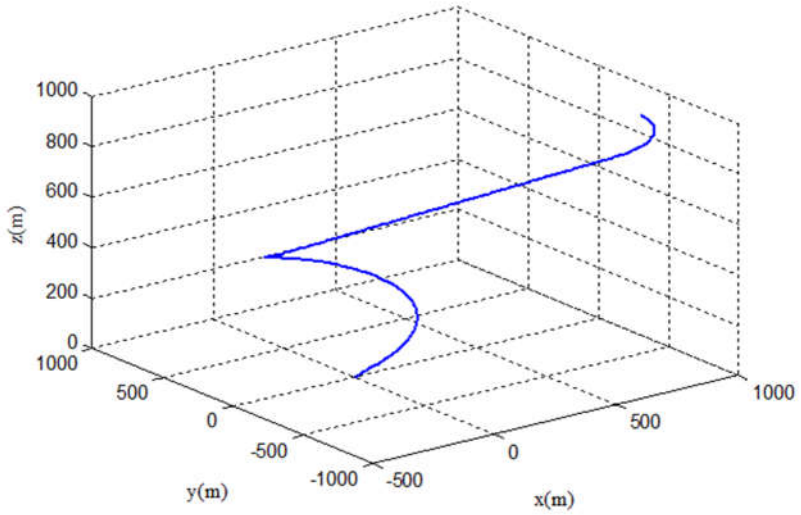

Figure 5. Three-dimensional trajectory under the state 1.

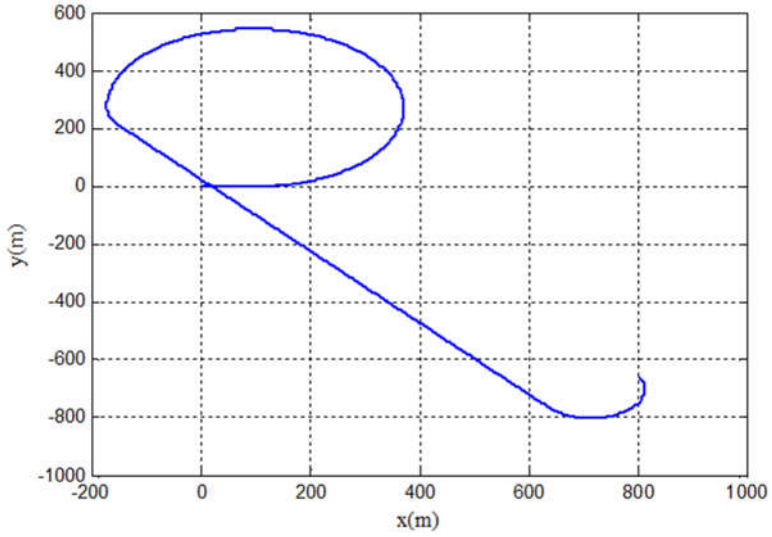

Figure 6. Horizontal trajectory under the state 1.

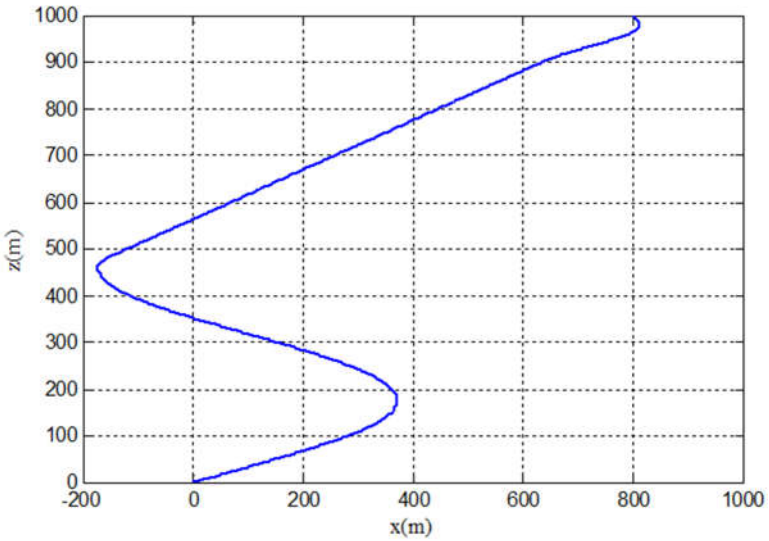

Figure 7. Longitudinal trajectory under the state 1.

Preprints (www.preprints.org) | NOT PEER-REVIEWED | Posted: 19 August 2022 doi:10.20944/preprints202208.0358.v1

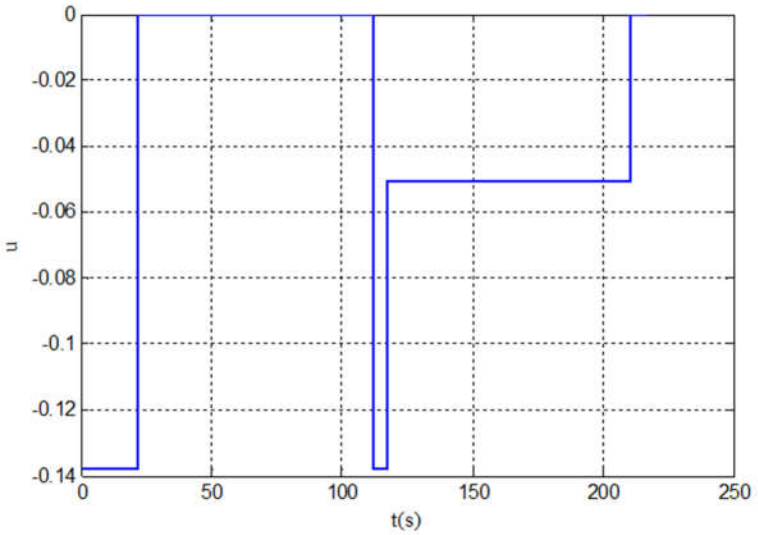

Figure 8. Control curve under the state 1.

Figures 5-7 are the effect diagrams of the trajectory planned by the new segmentation method. When the plane coordinates of the starting point of the parafoil airdrop system are at (800 m, -650 m), its position is at the lower right of the target point, and the starting flight direction is inconsistent with the direction of the target point. As can be seen from Figure 3, the planned trajectory firstly performs a turning flight to adjust the flight direction. The radian of the turning angle β_1 is about 2.9855 rad. After turning, the parafoil airdrop system enters the energy control area in the way of straight-line flight and minimum turning radius flight. In the energy control area, it makes a circling and height elimination flight with a radius $R_{ep} = 272.3363$ m, the turning flight is about 0.75 weeks, and the total radian β_3 is about 4.7124 rad. Finally, the airdrop system flies to the target point in a straight line along the tangent direction of the circle. The planned trajectory finally meets the requirement of aligning with the headwind to the landing target point.

5.2.2 Results of State 2

Figures 9-11 show the simulation results corresponding to state 2 in Table 2.

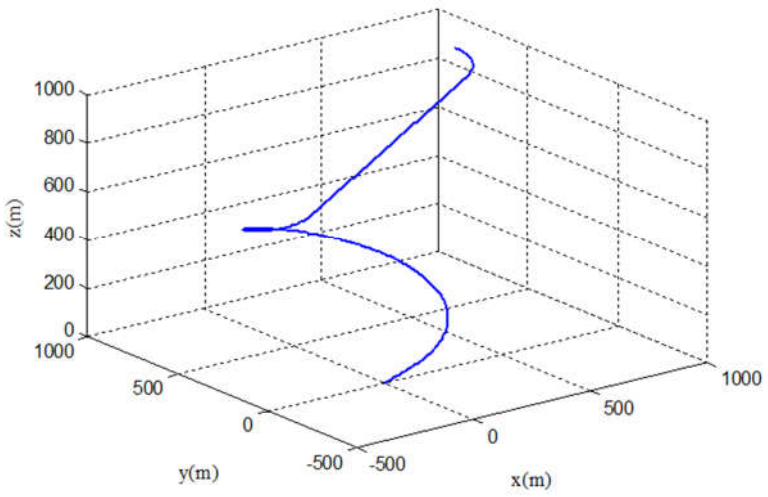

Figure 9. Three dimensional trajectory under the state 2.

Preprints (www.preprints.org) | NOT PEER-REVIEWED | Posted: 19 August 2022 doi:10.20944/preprints202208.0358.v1

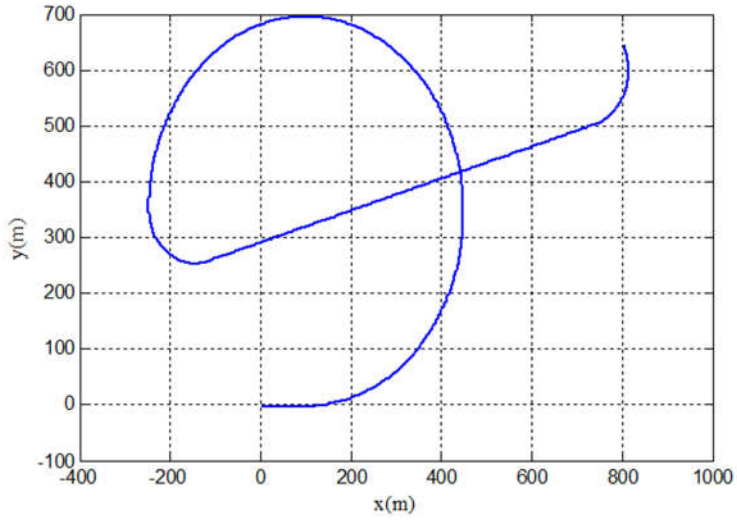

Figure 10. Horizontal trajectory under the state 2.

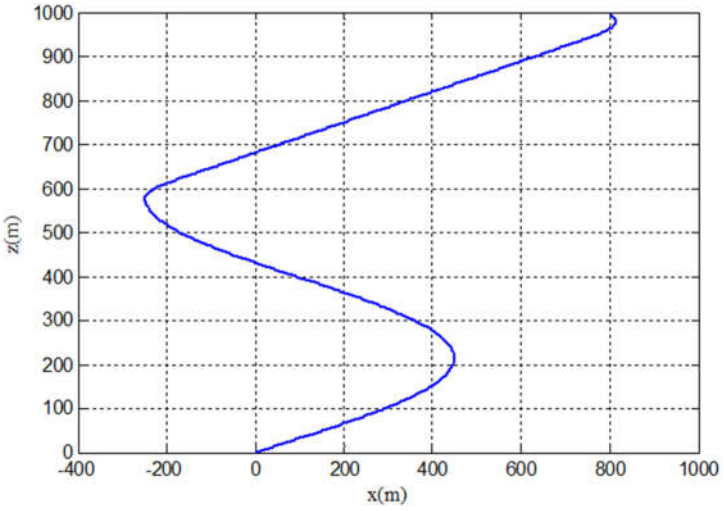

Figure 11. Longitudinal trajectory under the state 2.

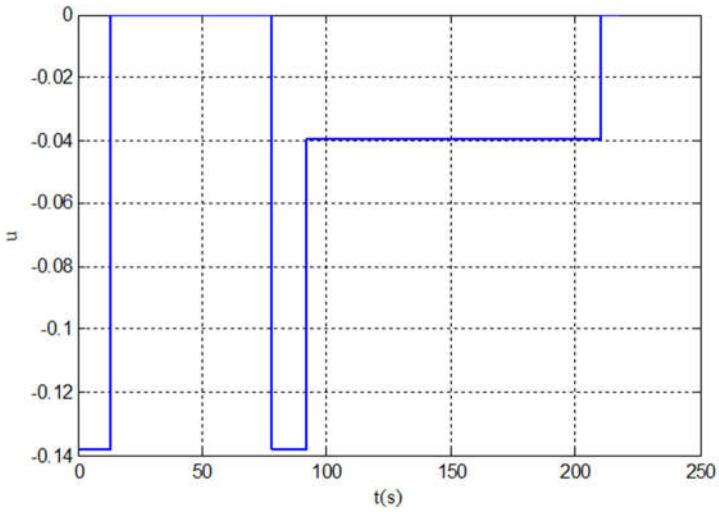

Figure 12. Control curve under the state 2.

Preprints (www.preprints.org) | NOT PEER-REVIEWED | Posted: 19 August 2022 doi:10.20944/preprints202208.0358.v1

In state 2, the starting point of the parafoil airdrop system is located at (800, 650, 1000), which is located at the upper right of the target point in the horizontal trajectory, and the airdrop height is consistent with state 1. The search algorithm is used to search for the optimal solution of the objective function, and the optimal entry point is located at $R_{ep} = 348.7353$ m, $\theta_{ep} = 3.0147$ rad. It can be seen from the planned trajectory curve that, similar to state 1, the whole trajectory is still composed of turning towards the target point, flying straight to the energy control area, circling and height elimination, and upwind alignment. At this time, β_1 is 1.8173 rad and β_3 is 4.6877 rad.

5.2.3. Results of State 3

Figures 13-15 are the effect diagrams of the trajectory planned by segments when the coordinates of the starting point are at (800 m, 650 m, 2000 ,).The entry point obtained by searching the optimal solution of the objective function is located at $R_{ep} = 421.2586$ m, $\theta_{ep} = 3.0147$ rad, and the angles of the two turning angles for adjusting the flight direction are $\beta_1 = 1.9473$ rad, $\beta_2 = 1.8447$ rad. The arc of the hovering height is $\beta_3 = 10.8687$ rad, which means the parafoil airdrop system hovers about 1.73 circles in the energy control area, and the elimination height is about 1526 m. The trajectory eventually enters the target point in the upwind direction.

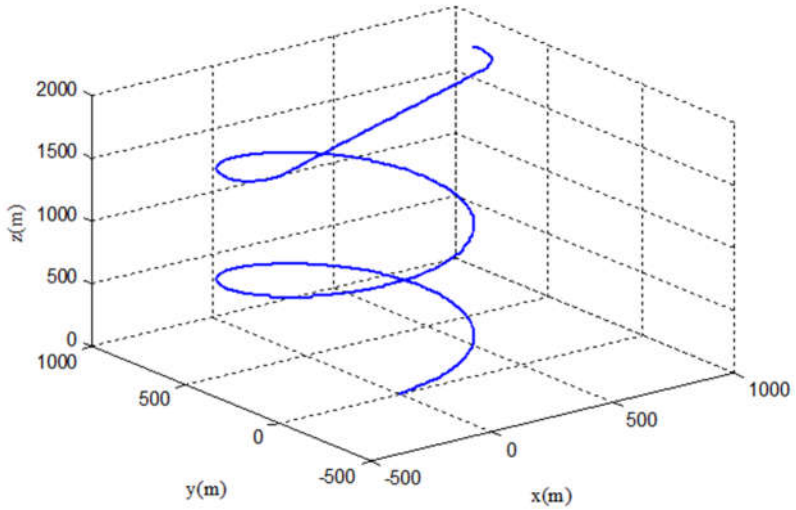

Figure 13. Three dimensional trajectory under the state 3.

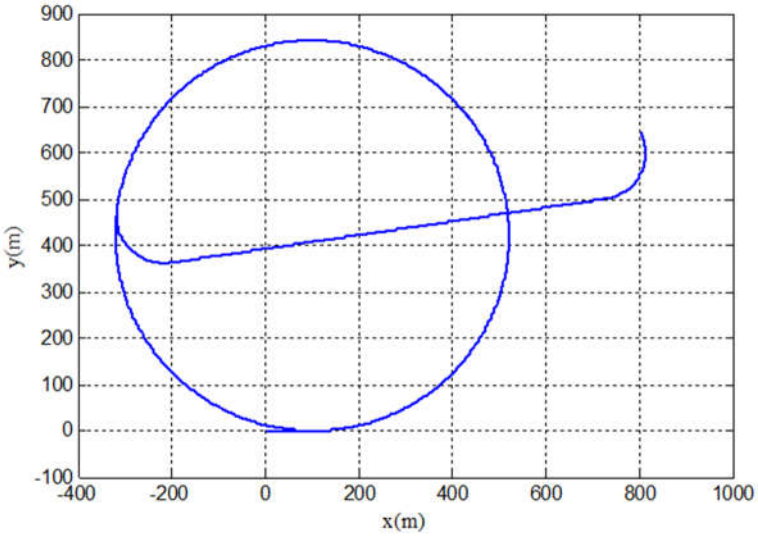

Figure 14. Horizontal trajectory (state 3).

Preprints (www.preprints.org) | NOT PEER-REVIEWED | Posted: 19 August 2022 doi:10.20944/preprints202208.0358.v1

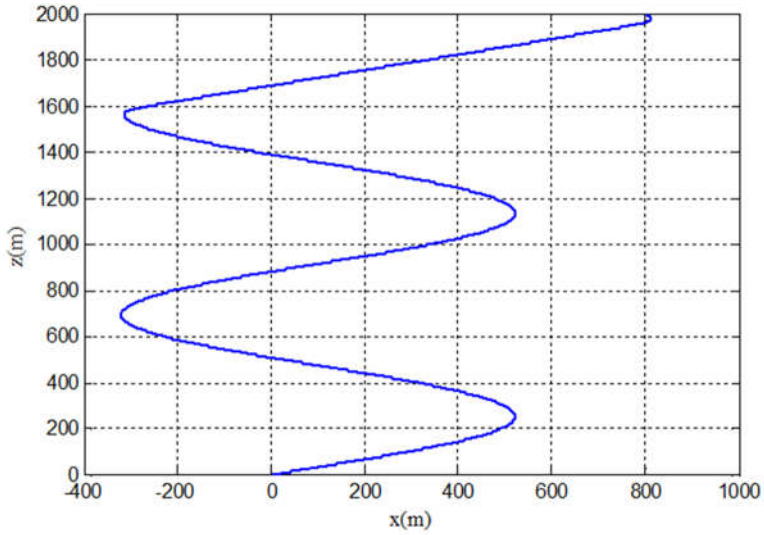

Figure 15. Longitudinal trajectory under the state 3.

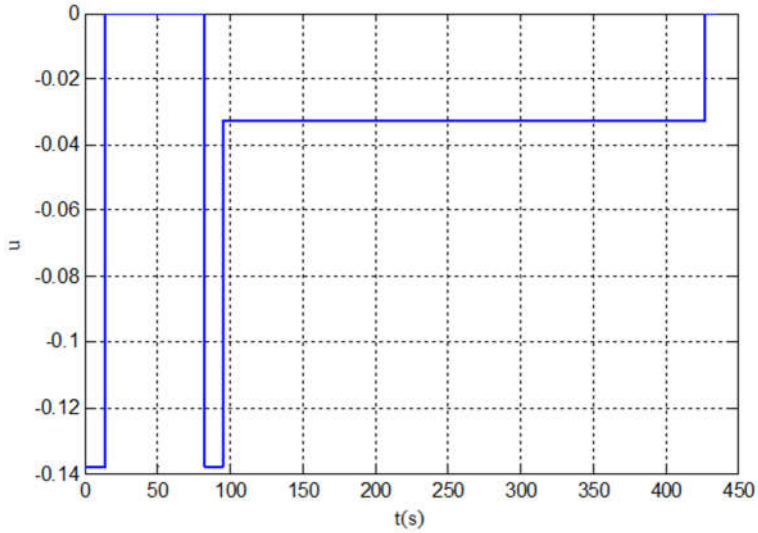

Figure 16. Control curve under the state 3.

Figure 8, Figure 10, and Figure 12 are the control curves under three different airdrop situations, respectively, corresponding to the trajectories planned in stages as shown in Figures 5, 9, and 13. It can be seen from the control curve that the control quantity corresponding to the homing trajectory planned by the segmental trajectory planning scheme proposed in this paper is a piecewise function whose value is less than zero, and the control quantity remains constant in the corresponding time period. This control is relatively simple in practical application, and the flight of the parafoil airdrop system is also relatively stable.

Table 3. Landing accuracy.

Initial state	Lateral error (m)	α_0(rad)
State 1	0.2684	3.14
State 2	0.0427	3.14
State 3	0.1615	3.14

Table 3 shows the landing accuracy of the three trajectories at the target point. It can be seen that the lateral error of the landing is small, and the landing direction is opposite

Preprints (www.preprints.org) | NOT PEER-REVIEWED | Posted: 19 August 2022 doi:10.20944/preprints202208.0358.v1

to the preset wind direction, which meets the design requirements. In addition, a large number of simulation experiments show that the optimization of the parameters of the trajectory optimization algorithm can be converged within 20 generations, showing good robustness.

Comparing the segmented trajectory under the third airdrop cases with the first two, it can be seen that due to the high position of the airdrop point in case 3 and the distance from the target point is farther than in cases 1 and 2, more time for circling and height elimination is required in the energy control area. On the contrary, if the airdrop altitude is too low and the distance from the target point is far, the system will not have enough time to achieve the target landing. Therefore, for the unpowered parafoil airdrop system, its airdrop position needs to be selected reasonably.

6. Discussion

Under the same conditions, when considering the landing accuracy of the target point, the accuracy of the trajectory planned by the method in this paper is basically the same order of magnitude compared with the existing classical segmented trajectory method. For example, when the coordinates of the starting point is at (800, 800, 2000) and the initial flight direction $\alpha_0 = -\pi/3$ rad, landing direction of the segmented trajectory planning strategy proposed in this paper is 3.14, and the landing error is 0.6685 m, which is about 0.3742 m higher than the accuracy of 1.0427 m in Ref [23].

Compared with the traditional classical segmented trajectory, the length of the glide trajectory before landing in the new scheme can be set freely according to the actual flight situation, which overcomes the defect that the length of the glide segment is affected by the radius of the parafoil circling flight circle, and has higher landing accuracy and safety. Therefore, the segmented trajectory optimization strategy of the parafoil airdrop system given in this paper is effective and feasible.

It should be pointed out that the trajectory planning scheme designed in this paper is the basic optimal design method for the autonomous homing trajectory of the parafoil. The trajectory planning problem with constraints such as obstacles and faults in the homing process is not within the scope of this paper.

7. Conclusions

In the design scheme of the segmented homing of the parafoil airdrop system, the landing target point or the position of executing the bird landing is usually set at the center of the circling flight area. This method has the problem that the length of the straight flight segment before landing is affected by the helix radius. When the radius calculated by the optimization parameters is small, the gliding flight segment of the parafoil will be shortened, which will bring difficulties to the bird landing operation, or even fail to perform the bird landing successfully, resulting in damage to the airdropped material. In this paper, the segmentation scheme is improved. The straight flight segment before landing is designed at the tangent position of the spiral height elimination circle, and its length can be freely controlled. Compared with the target point designed at the center position of the spiral height elimination circle, it avoids the problem that the length of the straight flight segment before landing is subject to the spiral radius and provides a guarantee for bird landing in terms of landing accuracy and safety.

Based on the verification needs of the new trajectory scheme, this paper establishes the point mass model of the parafoil airdrop system. On the basis of analyzing the flight characteristics of the parafoil airdrop system, the segmentation idea and design method of the new scheme are introduced, and the calculation method of each segment trajectory is analyzed. The calculation formula of the objective function and the constraint range of parameters R_{ep} and θ_{ep} are given. The application method and steps of the parameter optimization of the cuckoo optimization algorithm in the new scheme are introduced in detail. In order to fully verify the feasibility of the new scheme, the trajectory under dif-

ferent airdrop conditions is simulated in this paper. The results show that the correct trajectory can be successfully obtained under different initial conditions. Compared with the existing design schemes, the results show that the landing direction and accuracy of the new scheme can achieve ideal results, but the landing glide segment can be freely set and is no longer limited by the helix radius length, which proves the correctness and feasibility of the new trajectory design scheme. Moreover, the new scheme has the characteristics of simple control, high safety and easy realization in engineering. It is suitable for the trajectory planning of parafoil fixed-point airdrop system before autonomous homing and also provides a new reference for the landing flight of parafoil airdrop systems.

Author Contributions: Conceptualization, H.G. and T.J.; methodology, H.G.; software, H.G.; validation, H.G.; formal analysis, H.G. and T.J.; writing—original draft preparation, H.G.; writing—review and editing, H.G. and T.J. All authors have read and agreed to the published version of the manuscript.

Funding: This research was funded by the Natural Science Foundation of Anhui Province, China, grant number 1808085MF183 and Anhui University Top-notch Talents Academic Funding Project under grant number gxbjZD2020079.

Acknowledgments: The authors would like to express their sincerely thanks to all reviewers and editors for their help in improving the quality of this paper.

Conflicts of Interest: The authors declare no conflict of interest.

References

1. Yakimenko, O.A. Precision Aerial Delivery Systems: Modeling, Dynamics, and Control. AIAA-2015-248, 2015.
2. Sun, Q.L.; Li, Y.; Zheng, Y.M.; Tao, J.; Sun, H.; Sun, M.W.; Dehmer, M.; Chen, Z.Q. Trajectory tracking control of powered parafoil system based on sliding mode control in a complex environment. *Aerospace Science and Technology* **2022**, *122*, 107406.
3. Sun, H.; Sun, Q.L.; Zeng, X.Y.; Luo, S.Z.; Chen, Z.Q. Accurate Homing of Parafoil Delivery Systems based Glide-ratio Control. *IEEE Transactions on Aerospace and Electronic Systems* **2020**, *56*, 2374–2389.
4. Zhang, H.; Chen, Z.L.; Wei, J.B.; Su, L.J. Backstepping control method for path following of unmanned parafoil vehicle [J]. *Journal of Shanghai Jiang Tong University* **2016**, *50*, 1845–1852.
5. Jann, T. Advanced features for autonomous parafoil guidance, navigation and control, AIAA-2005-16428. 2005.
6. Mpanza, L.J.; Pedro, J.O. Optimised Tuning of a PID-Based Flight Controller for a Medium-Scale Rotorcraft. *Algorithms* **2021**, *14*, 178.
7. Tan, P.L.; Sun, Q.L.; Chen Z.Q. Application of active disturbance rejection control in trajectory tracking of powered paragoil system. *Journal of Zhejiang University (Engineering Science)* **2017**, *51*, 992–999.
8. Guo, Y.M.; Yan, J.G.; Wu, C.H.; Wu, C.; Xing, X. Autonomous homing design and following for parafoil/rocket system with high-altitude. *Journal of Intelligent & Robotic Systems* **2021**, *101*, 73.
9. Zhang, M.; Hu, W.; Ji, S.; Song, Q.; Gong, P.; Kong, L. Vision-Assisted Landing Method for Unmanned Powered Parachute Vehicle Based on Lightweight Neural Network. *IEEE Access* **2021**, *9*, 130981–130989.
10. Gao, H.T.; Jin, T.; Dehmer, M.; Emmert-streib, F.; Sun, Q.L.; Chen, Z.Q.; Xie G.M.; Zhou, Q. In-flight Wind Field Identification and Prediction of Parafoil Systems. *Applied Sciences* **2020**, *10*, 1958.
11. Long, X.; Sun, M.; Piao, M.; Chen, Z. Parameterized Trajectory Optimization and Tracking Control of High Altitude Parafoil Generation. *Energies* **2021**, *14*, 7460.
12. Omar, H.M. Optimal Geno-Fuzzy Lateral Control of Powered Parachute Flying Vehicles. *Aerospace* **2021**, *8*, 400.
13. García-Beltrán, C.; Miranda-Araujo, E.; Guerrero-Sanchez, M.; Valencia-Palomo, G.; Hernández-González, O.; Gómez-Peñate, S. Passivity-Based Control Laws for an Unmanned Powered Parachute Aircraft. *ASIAN JOURNAL OF CONTROL* **2021**, *23*, 287–296.
14. Tao, J.; Sun, Q.L.; Zhu, E.L.; Chen, Z.Q.; He, Y.P. Genetic algorithm based homing trajectory planning of parafoil system with constraints. *Journal of Central South University (Science and Technology)* **2017**, *48*, 404–410.
15. Sun, H.; Sun, Q.L.; Luo, S.Z.; Chen, Z.Q.; Wu, W.N.; Tao, J.; He, Y.P. In-flight compound homing methodology of parafoil delivery systems under multiple constraints. *Aerospace Science and Technology* **2018**, *79*, 85–104.
16. Zhang, L.M; Gao, H.T.; Chen, Z.Q.; Sun, Q.L.; Zhang, X.H. Multi-objective global optimal parafoil homing trajectory optimization via Gauss pseudospectral method. *Nonlinear Dynamics* **2013**, *72*, 1–8.
17. Gao, H.T.; Zhang, L.M; Sun, Q.L.; Sun, M.W.; Chen, Z.Q.; Kang, X.F. Fault-tolerance design of homing trajectory for parafoil system based on pseudo-spectral method. *Control Theory & Applications* **2013**, *30*, 702–708.
18. Chen, Z.M.; Guo, D.Y.; Lin, Y. A Deep Gaussian Process-Based Flight Trajectory Prediction Approach and Its Application on Conflict Detection. *Algorithms* **2020**, *13*, 293
19. Luo, S.Z.; Sun, Q.L.; Tan, P.L.; et al. Trajectory planning of parafoil system with intricate constraints based on Gausspseudospectral method. *Acta Aeronautica et Astronautica Sinica* **2017**, *38*, 320363.

20. Sun, H.; Luo, S.Z.; Sun, Q.L.; Tao, J.; Luo, H. Trajectory optimization for parafoil delivery system considering complicated dynamic constraints in high-order model. *Aerospace Science and Technology* **2020**, *98*, 105631.
21. Sun, H.; Sun, Q.L.; Chen, Z.Q.; Tao, J. Trajectory planning for parafoil system considering dynamic constraints in complicated environment. *Aerospace Science and Technology* **2021**, *42*, 324301.
22. Jiang, H.C.; Liang, H.Y.; Zeng, D.T.; Yan, J. Design of the optimal homing trajectoryof a parafoil system considering threat avoidance. *Journal of Harbin Engineering University* **2016**, *37*, 995–962.
23. Gao, H.T.; Tao, J.; Sun, Q.L.; Chen, Z.Q. Design and optimization in multiphase homing trajectory of parafoil system [J]. *Journal of Central South University* **2016**, *23*, 1416–1426.
24. Chen, Q.; Zhao, M.; Li, Y.H.; He, Z.Y. Optimal segment constant trajectory planning for parafoil system based on gradient descent method. *Acta Aeronautica et Astronautica Sinica* **2020**, *41*, 324226.
25. Gao, H.T. Research on Control and Autonomous Homing Trajectory Planning of Parafoil System. PhD, Nankai University, Tianjiin, China, 2014.
26. Lee, S.J.; Jr, J.C.; Jr, A.A. An Autonomous Recovery System for High Altitude Payloads by Using a Parafoil. In Proceedings of the AIAA Atmospheric Flight Mechanics Conference, Atlanta, USA, 16-20 June 2014.
27. Yang, X.S.; Suash, D. Engineering optimisation by cuckoo search. *Int'l Journal of Mathematical Modelling & Numerical Optimisation* **2010**, *1*, 330–343.
28. Feng, Y.; Zhou, J.Z.; Mo, L.; Wang, C.; Yuan, Z.; Wu, J. A Gradient-Based Cuckoo Search Algorithm for a Reservoir-Generation Scheduling Problem. *Algorithms* **2018**, *11*, 36
29. Zhang; Y.Y.; Jin, Z.G. An improved cuckoo search for multimodal optimization problems. *Journal of Harbin Institute of Technology* **2019**, *51*, 89–99.
30. Fu, W.Y. Cuckoo search algorithm with gravitational acceleration mechanism. *Journal of Software* **2021**, *32*, 1480–1494.